

RESEARCH ARTICLE

Stable numerics for finite-strain elasticity

Rezgar Shakeri¹ | Leila Ghaffari² | Karen Stengel² | Jeremy L. Thompson² | Jed Brown^{*2}¹Department of Civil, Environmental, and Architectural Engineering, University of Colorado Boulder, CO, United States²Department of Computer Science, University of Colorado Boulder, CO, United States

Correspondence

*Jed Brown 

Email: jed.brown@colorado.edu

Funding Information

This research was supported by the U.S. Department of Energy, Office of Science, Office of Advanced Scientific Computing Research, applied mathematics program and by the National Nuclear Security Administration, Predictive Science Academic Alliance Program (PSAAP) under Award Number DE-NA0003962.

Abstract

A backward stable numerical calculation of a function with condition number κ will have a relative accuracy of $\kappa\epsilon_{\text{machine}}$. Standard formulations and software implementations of finite-strain elastic materials models make use of the deformation gradient $\mathbf{F} = \mathbf{I} + \partial\mathbf{u}/\partial\mathbf{X}$ and Cauchy-Green tensors. These formulations are not numerically stable, leading to loss of several digits of accuracy when used in the small strain regime, and often precluding the use of single precision floating point arithmetic. We trace the source of this instability to specific points of numerical cancellation, interpretable as ill-conditioned steps. We show how to compute various strain measures in a stable way and how to transform common constitutive models to their stable representations, formulated in either initial or current configuration. The stable formulations all provide accuracy of order $\epsilon_{\text{machine}}$. In many cases, the stable formulations have elegant representations in terms of appropriate strain measures and offer geometric intuition that is lacking in their standard representation. We show that algorithmic differentiation can stably compute stresses so long as the strain energy is expressed stably, and give principles for stable computation that can be applied to inelastic materials.

KEYWORDS

finite strain, hyperelasticity, numerical stability, conditioning

1 | INTRODUCTION

Errors in computational mechanics are attributable to three sources: continuum model specification (materials, geometry, boundary conditions), discretization (finite elements), and numerical. When working in double precision with direct solvers, the first two typically dominate numerical errors and stable numerics are overlooked beyond linear algebra. Meanwhile, single precision is widely considered to be insufficient for finite-strain implicit analysis and practitioners opt for distinct small-strain formulations due to a combination of instability and perceived cost of finite-strain formulations in small-strain regimes. This shifts a cognitive burden to the practitioner who must confirm that the small-strain formulations are valid, and is problematic for high-contrast materials in which finite strains and infinitesimal strains are present within the same analysis. In this paper, we demonstrate the instability in standard formulations for hyperelasticity and present intuitive (and mathematically equivalent) reformulations that are stable, enabling finite-strain analysis at all strains and opening the door for reduced precision analysis.

In floating point arithmetic, $\epsilon_{\text{machine}} = \sup_x |\text{fl}(x) - x|/|x|$ is the maximum error incurred rounding a real number x to its nearest floating point representation $\text{fl}(x)$. (We assume x is within the exponent range and will not discuss overflow/underflow/denormals.) Typical values of $\epsilon_{\text{machine}}$ are $2^{-53} \approx 10^{-16}$ for IEEE-754 double precision and $2^{-24} \approx 6 \cdot 10^{-8}$ for single precision. Elementary math operators \otimes (standing for addition, subtraction, multiplication, or division) and special functions behave as “exact arithmetic, correctly rounded”, $x \otimes y = \text{fl}(x \otimes y)$ ¹, thus guaranteeing $|x \otimes y - x \otimes y|/|x \otimes y| \leq \epsilon_{\text{machine}}$.

With such strong guarantees from elementary operations, we might hope that $(x \otimes y) \otimes z$ is also accurate to $\epsilon_{\text{machine}}$, but also, this is not true. An illustrative example is computing $(x + 1) - 1$. For $x = 10^{-16}$ in double precision, $x \oplus 1 = 1$, thus $(x \oplus 1) \ominus 1 = 0$ has a relative error of 1, which is much larger than $\epsilon_{\text{machine}}$. For larger values of x , we observe the stair-step effect in Figure 1. The first operation incurred a relative error smaller than $\epsilon_{\text{machine}}$ and the second operation was exact, so where can we place blame for the catastrophic cancellation error? To shed light on this, we consider the condition number of a differentiable function

$f(x)$, defined as

$$\kappa_f(x) = \left| \frac{\partial f}{\partial x} \right| \frac{|x|}{|f(x)|}. \quad (1)$$

The first operation $x + 1$ has a condition number of 1 while the second has enormous condition number. An numerical algorithm \tilde{f} for evaluating the continuum function f is called *backward stable* if it computes the exact answer to a problem with almost the given inputs, i.e., $\tilde{f}(x) = f(x')$ for some nearby x' satisfying $|x' - x|/|x| < c\epsilon_{\text{machine}}$ for a small constant c . Backward stable algorithms satisfy the forward error bound¹

$$\frac{|\tilde{f}(x) - f(x)|}{|f(x)|} < c\kappa_f(x)\epsilon_{\text{machine}}. \quad (2)$$

Furthermore, this bound composes when the underlying functions are well-conditioned: if \tilde{f} and \tilde{g} are both backward stable algorithms, then

$$\frac{|\tilde{f}(\tilde{g}(x)) - f(g(x))|}{|f(g(x))|} < c\kappa_f(g(x))\kappa_g(x)\epsilon_{\text{machine}}.$$

Note that if $\kappa_{f \circ g}(x) \approx \kappa_f(g(x))\kappa_g(x)$, this is the bound we would get for $\tilde{f} \circ \tilde{g}$ as a backward stable algorithm. As a corollary, any calculation constructed from backward stable parts (such as elementary arithmetic) that exhibits large errors must have ill-conditioned steps. An intuitive and quantifiable strategy for designing stable algorithms is to ensure that every step is as well-conditioned as possible.

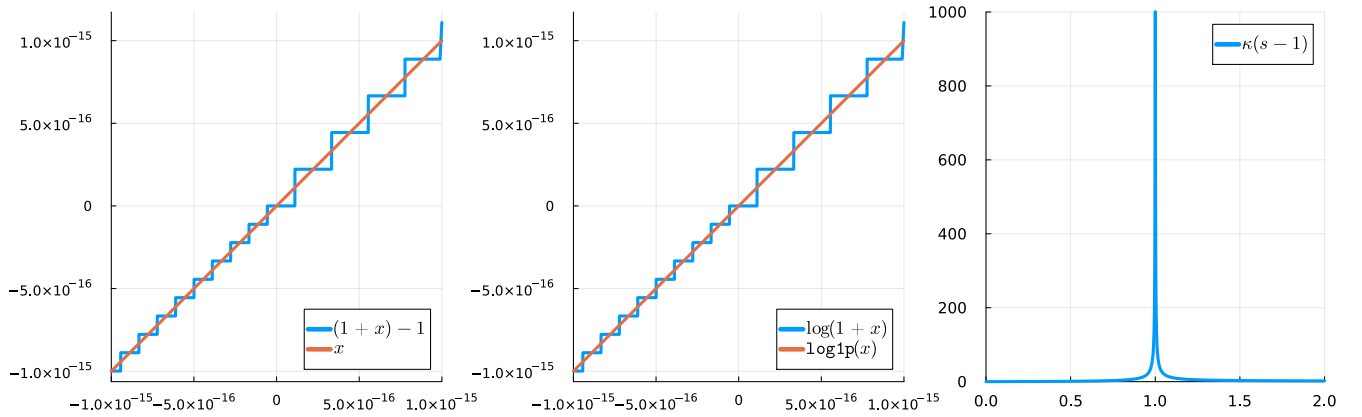


FIGURE 1 The stair-step patterns illustrate numerical instability evaluating in $(1+x) - 1$ (left) and $\log(1+x)$ (center). When evaluating $(1+x) - 1$, a small relative error is incurred in the well-conditioned operation $s := 1+x$, and that error becomes a large relative error because $s - 1$ has unbounded condition number as $s \rightarrow 1$ (right), despite this operation being computed exactly in floating point arithmetic.

We now turn our attention to representative functions in solid mechanics. Most strain-energy functions and corresponding stress models in hyperelasticity contain expressions like $\log(1+x)$ or $\exp(x) - 1$, which are numerically unstable expressions when $x \approx 0$. Numerical analysts proposed^{2,3}

$$\text{log1p}(x) = \log(1+x)$$

$$\text{expm1}(x) = \exp(x) - 1,$$

which gives high precision value for small values of x ; these are in most core math libraries since C99. Figure 1 shows the x , $(1+x) - 1$ and $\log(1+x)$, $\text{log1p}(x)$ functions around 0. In both cases, large relative error is incurred by an algorithmic step that maps values near 1 to values near 0 via a function of derivative about 1, leading to unbounded condition number (1). Note that $\log(1+x)$ and $\exp(x) - 1$ are both well conditioned, but their direct evaluation is numerically unstable due to an ill-conditioned step. We surveyed many open source finite element analysis packages and found that all contain numerically unstable formulations at some point due to phenomena explained above.

TABLE 1 A stable constitutive implementation requires stable computation of strain \mathbf{E} , $J = |\mathbf{F}|$, $\log J$, and shear expressions involving first and second invariants of \mathbf{C} . Unstable formulations are widespread in books and software, with Ratel having the only stable formulation we are aware of.

Software/book	stable strain \mathbf{E}	stable J	stable $\log J$	stable constitutive equation
FEAP ⁵	✓	–	–	–
FEBio ⁸	–	–	–	–
Abaqus ⁷	–	–	–	–
MOOSE ¹⁰	–	–	–	–
Albany-LCM ¹¹	–	–	–	–
LifeV ¹²	–	–	–	–
MoFEM ⁹	–	–	–	–
Ratel ¹³	✓	✓	✓	✓
Holzappel ¹⁴	–	–	–	–
Wriggers ⁴	–	–	–	–

1.1 | Finite-strain mechanics

Let \mathbf{X} be the reference configuration and $\mathbf{x} = \mathbf{X} + \mathbf{u}$ be the current configuration expressed in terms of the displacement \mathbf{u} . Wriggers⁴ discusses the displacement gradient

$$\mathbf{H} = \frac{\partial \mathbf{u}}{\partial \mathbf{X}}$$

and mentions that the Green-Lagrange strain can be expressed as

$$\mathbf{E}(\mathbf{H}) = \frac{1}{2}(\mathbf{H} + \mathbf{H}^T + \mathbf{H}^T \mathbf{H}) \quad (3)$$

“in analytical investigations”, but notes “This is actually not necessary when a numerical approach is applied.” The usual presentation defines the deformation gradient $\mathbf{F} = \mathbf{I} + \mathbf{H}$ and proceeds to the right Cauchy-Green tensors $\mathbf{C} = \mathbf{F}^T \mathbf{F}$ and $\mathbf{E} = \frac{1}{2}(\mathbf{C} - \mathbf{I})$. At small strain, \mathbf{E} is small despite \mathbf{F} and \mathbf{C} being of order 1, leading to instability as in the examples above. For stable compressible formulations, one must also formulate expressions involving $J = |\mathbf{F}|$ and the first and second invariants of \mathbf{C} in a stable way.

Developers of FEAP⁵ observed numerical stability issues when applying the standard approach at small strains and have begun to favor working directly with the displacement gradient \mathbf{H} ⁶ but did not complete a stable compressible hyperelastic formulation. The Abaqus UMAT⁷ interface provides the deformation gradient \mathbf{F} and a strain increment, but does not provide direct access to the displacement gradient \mathbf{H} or nonlinear strain tensor, therefore numerical cancellation is inevitable when small strains appear within large strain formulations. FEBio⁸, a nonlinear finite element package for biomechanical applications, uses the deformation gradient \mathbf{F} even for defining the linear strain tensor. Moreover, they offer a varieties of hyperelasticity models that contains the subtraction, which leads to loss of significance when the problem is in a small deformation regime. MoFEM⁹, an open source library for solving complex physics problems, uses the standard formulation given in continuum mechanics text books to describe the stress-strain relation of material. This constitutive formulation contains $\log J$ function, leading to instability when $J \approx 1$. Similarly, the Multiphysics Object-Oriented Simulation Environment (MOOSE)¹⁰ defines, for example, the Neo-Hookean model using the standard (numerically unstable) formulation. Albany-LCM¹¹, a finite element code for analysis of multiphysics problem on unstructured grid expresses the hyperelastic models in terms of $J^2 - 1$, which leads to catastrophic cancellation when $J \approx 1$. Table 1 summarizes the stability properties of formulations used in well-known text books and production software.

The paper proceeds as follows: section 2 develops stable formulations for common hyperelastic models in coupled and decoupled (isochoric and volumetric split), section 3 demonstrates that stable stress expressions can be derived using algorithmic differentiation (AD) so long as care is taken in the strain energy formulation, and section 4 concludes with outlook toward inelastic models. Details of the numerical procedure for evaluating stability are given in Appendix A. All figures exhibited here are created using the open source Julia programming language. Comprehensive numerical experiments and figures are provided in the executable supplement¹⁵ for those readers who are interested in exploring of all given formulations here. While this study presents some of the most well-known hyperelastic models and their stable formulation, the approach is general and we provide guidance for applying it to other material models.

2 | CONSTITUTIVE EQUATIONS

The constitutive behavior for hyperelastic materials is characterized by a strain energy density function ψ . For isotropic materials in initial configuration, ψ is typically defined by either the principal invariants $\{\mathbb{I}_1, \mathbb{I}_2, \mathbb{I}_3\}$ of right Cauchy-Green tensor $\mathbf{C} = \mathbf{F}^T \mathbf{F}$ or the principal stretches $\{\lambda_1, \lambda_2, \lambda_3\}$ of the SPD matrix \mathbf{U} where $\mathbf{R}\mathbf{U} = \mathbf{F}$ is the polar decomposition. In the following we discuss the most common coupled and decoupled representation of the strain energies and the associated constitutive equations that are employed frequently in the literature.

2.1 | Coupled strain energy

Coupled strain energy functionals ψ are written in terms of invariants without an isochoric-volumetric split. In the linear regime, this corresponds to use of shear modulus μ and first Lamé parameter λ , with the standard (not deviatoric) infinitesimal strain tensor $\boldsymbol{\varepsilon}$. For the general form of coupled strain energy

$$\psi(\mathbf{C}) = \psi(\mathbb{I}_1, \mathbb{I}_2, \mathbb{I}_3), \quad (4)$$

with the invariants

$$\begin{aligned} \mathbb{I}_1(\mathbf{C}) &= \text{trace } \mathbf{C}, \\ \mathbb{I}_2(\mathbf{C}) &= \frac{1}{2} (\mathbb{I}_1^2 - \mathbf{C} : \mathbf{C}) \\ \mathbb{I}_3(\mathbf{C}) &= |\mathbf{C}|. \end{aligned} \quad (5)$$

we can determine the constitutive equations by taking the gradient of strain energy as

$$\mathbf{S} = \frac{\partial \psi}{\partial \mathbf{E}} = 2 \frac{\partial \psi}{\partial \mathbf{C}} = 2 \sum_{i=1}^3 \frac{\partial \psi}{\partial \mathbb{I}_i} \frac{\partial \mathbb{I}_i}{\partial \mathbf{C}}, \quad (6)$$

where \mathbf{S} is the general form of the stress relation in initial configuration and

$$\begin{aligned} \frac{\partial \mathbb{I}_1}{\partial \mathbf{C}} &= \mathbf{I}_3, \\ \frac{\partial \mathbb{I}_2}{\partial \mathbf{C}} &= \mathbb{I}_1 \mathbf{I}_3 - \mathbf{C} \\ \frac{\partial \mathbb{I}_3}{\partial \mathbf{C}} &= \mathbb{I}_3 \mathbf{C}^{-1}. \end{aligned} \quad (7)$$

In the following we introduce the stable formulation for two well-known hyperelastic constitutive equations.

2.1.1 | Neo-Hookean model

One of the simplest hyperelastic models is the Neo-Hookean model, given by

$$\psi(\mathbf{C}) = \frac{\lambda}{4} (J^2 - 1 - 2 \log J) - \mu \log J + \frac{\mu}{2} (\mathbb{I}_1 - 3) \quad (8)$$

where $J = |\mathbf{F}| = \sqrt{|\mathbf{C}|}$. The first term is a convex choice satisfying limit conditions^{4,16} while the second is a structural necessity for coupled strain energy formulations. The second Piola-Kirchhoff stress is derived according to (7)

$$\mathbf{S} = 2 \frac{\partial \psi}{\partial \mathbf{C}} = \frac{\partial \psi}{\partial \mathbf{E}} = \frac{\lambda}{2} (J^2 - 1) \mathbf{C}^{-1} + \mu (\mathbf{I} - \mathbf{C}^{-1}), \quad (9)$$

where $\mathbf{C} = \mathbf{I} + 2\mathbf{E}$. Both terms are numerically unstable expressions at small strain ($\mathbf{C} \approx \mathbf{I}$), but the first is also unstable when $J \approx 1$ at large strain, a condition that is prevalent for nearly incompressible materials. Similar to `log1p`, we need a formulation that avoids direct computation of J in $J^2 - 1 = (J - 1)(J + 1)$.

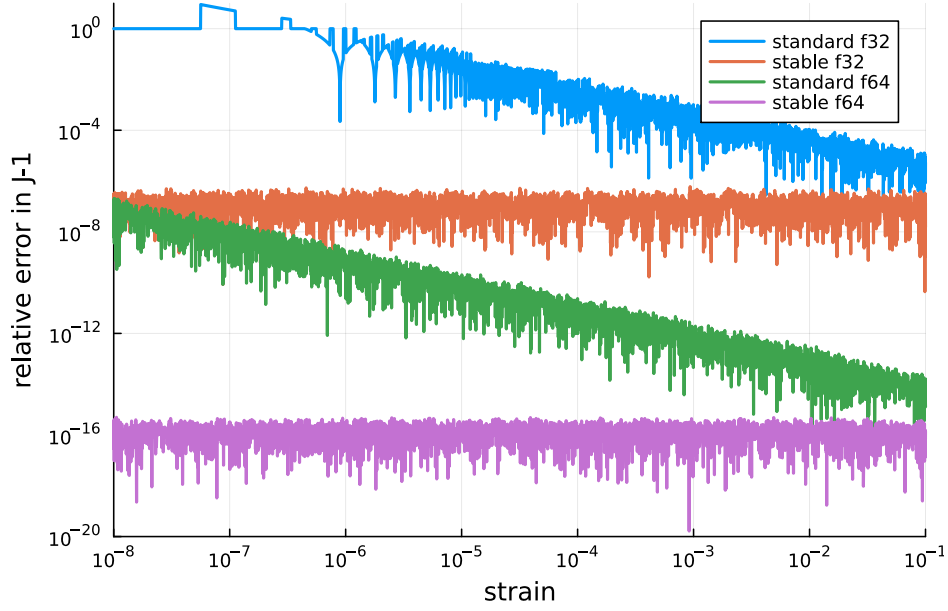


FIGURE 2 Relative error of standard computation of $J - 1$ and its stable way \mathcal{J}_{-1}

Consider the 2-dimensional case

$$\mathbf{F} = \mathbf{I} + \mathbf{H} = \mathbf{I} + \nabla_{\mathbf{x}} \mathbf{u} = \begin{bmatrix} 1 + u_{1,1} & u_{1,2} \\ u_{2,1} & 1 + u_{2,2} \end{bmatrix},$$

and let $\mathcal{J}_{-1} = J - 1$ be computed by the stable expression

$$\mathcal{J}_{-1} = u_{1,1} + u_{2,2} + u_{1,1}u_{2,2} - u_{1,2}u_{2,1}. \quad (10)$$

Remark 1. Ideally, one would like a proof of backward stability for every constitutive model, but doing so is tedious and we believe offers no great insight. In light of (2), it is revealing to plot the forward relative error and observe that stable algorithms provide errors that are uniformly of order $\epsilon_{\text{machine}}$ (sometimes written “in $O(\epsilon_{\text{machine}})$ ”) independent of the input argument \mathbf{H} (or a strain). There is a caveat: in the case of tiny perturbations of a pure rotation $\mathbf{H} \approx \mathbf{Q} - \mathbf{I}$ for an orthogonal matrix \mathbf{Q} , the strain is nearly zero and thus stress will also be nearly zero. For example, the Green-Lagrange strain $\mathbf{E}(\mathbf{H}) = \frac{1}{2}(\mathbf{F}^T \mathbf{F} - \mathbf{I}) \approx \frac{1}{2}(\mathbf{Q}^T \mathbf{Q} - \mathbf{I}) = \mathbf{0}$ is a function with unbounded condition number, thus even a backward stable algorithm such as (3) will have unbounded error in \mathbf{E} . One might consider high/mixed precision or alternative state variables \mathbf{u} that make strain a well-conditioned function of the state if a problem requires small-strain stability for large motions of floating bodies. While we consider \mathbf{H} as the input in our numerical experiments (to be agnostic over strain measures), we will not construct cases of nearly-pure rotations.

Remark 2. Apart from the incompressible limit, hyperelastic constitutive models are well-conditioned, thus (2) ensures the error will be in $O(\epsilon_{\text{machine}})$. Although various displacement-only formulations are common in engineering practice, mixed methods are necessary for well-conditioned finite element formulations in the incompressible limit.

Using a 3-dimensional analog of (10) described in Appendix A and numerical procedure explained therein, Figure 2 shows that the relative error in \mathcal{J}_{-1} is $O(\epsilon_{\text{machine}})$ independent of the magnitude of the displacement gradient \mathbf{H} and strain, while $J - 1$ loses digits of accuracy at small strain. Replacing $J^2 - 1$ with $\mathcal{J}_{-1}(\mathcal{J}_{-1} + 2)$ is sufficient to stabilize the first term of (9).

In some constitutive models, $\log J$ appears directly in the expression for \mathbf{S} , and also has a huge condition number $\kappa_{\log}(J) = 1/\log J$ when $J \approx 1$. In such cases, one naturally achieves stability via

$$\log J = \log_{10}(\mathcal{J}_{-1}). \quad (11)$$

The Neo-Hookean constitutive equation (9) is also unstable due to cancellation in the second term when $\mathbf{C}^{-1} \approx \mathbf{I}$, and it can be fixed by replacing $\mathbf{I} - \mathbf{C}^{-1} = \mathbf{C}^{-1}(\mathbf{C} - \mathbf{I}) = 2\mathbf{C}^{-1}\mathbf{E}$. Thus, an equivalent stable form of (9) is

$$\mathbf{S} = \frac{\lambda}{2} \mathbb{J}_{-1} (\mathbb{J}_{-1} + 2) \mathbf{C}^{-1} + 2\mu \mathbf{C}^{-1} \mathbf{E}. \quad (12)$$

The relative error in \mathbf{S} using the standard (9) and stable (12) expressions yields a figure indistinguishable from Figure 2. Although we elide figures for each constitutive model and stress, the supplement¹⁵ contains numerical demonstration that every expression we call unstable or stable exhibits errors indistinguishable from the corresponding line in Figure 2.

The Neo-Hookean constitutive model can also be evaluated in current configuration, classically written in terms of J and the left Cauchy-Green tensor $\mathbf{b} = \mathbf{F}\mathbf{F}^T$. One can derive an expression for a current configuration stress (we use Kirchhoff stress $\boldsymbol{\tau}$) starting with a strain energy density $\psi(\mathbf{b})$ or (equivalently) pushing \mathbf{S} of (9) forward via

$$\boldsymbol{\tau} = \mathbf{F}\mathbf{S}\mathbf{F}^T = \frac{\lambda}{2} (J^2 - 1) \mathbf{I} + \mu (\mathbf{b} - \mathbf{I}). \quad (13)$$

A stable form analogous to (12) is

$$\boldsymbol{\tau} = \frac{\lambda}{2} \mathbb{J}_{-1} (\mathbb{J}_{-1} + 2) \mathbf{I} + 2\mu \mathbf{e}, \quad (14)$$

where we call $\mathbf{e} = \frac{1}{2}(\mathbf{b} - \mathbf{I}) = \frac{1}{2}(\mathbf{H} + \mathbf{H}^T + \mathbf{H}\mathbf{H}^T)$ the Green-Euler strain tensor. (It is the $n = 2$ current configuration Seth-Hill strain measure¹⁴.)

2.1.2 | Mooney-Rivlin model

Compared to the Neo-Hookean model (8), the coupled energy function for Mooney-Rivlin model depends on the additional invariant $\mathbb{I}_2(\mathbf{C}) = \frac{1}{2} (\mathbb{I}_1^2(\mathbf{C}) - \mathbf{C}:\mathbf{C})$ where $\mathbf{C}:\mathbf{C} = \text{trace}(\mathbf{C}^T \mathbf{C})$ is the Frobenius inner product. The coupled Mooney-Rivlin strain energy is given by¹⁴

$$\psi(J, \mathbf{C}) = \frac{\lambda}{4} (J^2 - 1 - 2 \log J) - (\mu_1 + 2\mu_2) \log J + \frac{\mu_1}{2} (\mathbb{I}_1(\mathbf{C}) - 3) + \frac{\mu_2}{2} (\mathbb{I}_2(\mathbf{C}) - 3), \quad (15)$$

where μ_1 and μ_2 are parameters that must be experimentally determined and $\mu = \mu_1 + \mu_2$ is the shear modulus in the linear regime. The second Piola-Kirchhoff tensor is

$$\mathbf{S} = \frac{\lambda}{2} (J^2 - 1) \mathbf{C}^{-1} + \mu_1 (\mathbf{I} - \mathbf{C}^{-1}) + \mu_2 (\mathbb{I}_1(\mathbf{C}) \mathbf{I} - 2\mathbf{C}^{-1} - \mathbf{C}). \quad (16)$$

Similar to the Neo-Hookean model, we write the stable form in terms of Green-Lagrange strain,

$$\mathbf{S} = \frac{\lambda}{2} \mathbb{J}_{-1} (\mathbb{J}_{-1} + 2) \mathbf{C}^{-1} + 2(\mu_1 + 2\mu_2) \mathbf{C}^{-1} \mathbf{E} + 2\mu_2 (\mathbb{I}_1(\mathbf{E}) \mathbf{I} - \mathbf{E}). \quad (17)$$

In addition, the Kirchhoff stress tensor for Mooney-Rivlin in current configuration is classically written

$$\boldsymbol{\tau} = \frac{\lambda}{2} (J^2 - 1) \mathbf{I} + \mu_1 (\mathbf{b} - \mathbf{I}) + \mu_2 (\mathbb{I}_1(\mathbf{b}) \mathbf{b} - 2\mathbf{I} - \mathbf{b}^2) \quad (18)$$

and its stable form in terms of Green-Euler strain is

$$\boldsymbol{\tau} = \frac{\lambda}{2} \mathbb{J}_{-1} (\mathbb{J}_{-1} + 2) \mathbf{I} + 2(\mu_1 + 2\mu_2) \mathbf{e} + 2\mu_2 (\mathbb{I}_1(\mathbf{e}) \mathbf{I} - \mathbf{e}) \mathbf{b}. \quad (19)$$

2.2 | Decoupled strain energy

Decoupled strain energy formulations decompose the strain into volumetric and deviatoric parts. In the linear regime, such formulations use the shear modulus μ and bulk modulus k , with the deviatoric strain $\boldsymbol{\varepsilon}' = \boldsymbol{\varepsilon} - \frac{1}{3}(\text{trace } \boldsymbol{\varepsilon}) \mathbf{I}$. In the case of rubber-like materials, the bulk modulus k is orders of magnitude larger than the shear modulus, $k \gg \mu$. For finite strain, the strain

energy function is split into volumetric and isochoric (volume-preserving) parts. The first step is multiplicative decomposition of the deformation gradient as

$$\mathbf{F} = (J^{1/3} \mathbf{I}) \bar{\mathbf{F}} = J^{1/3} \bar{\mathbf{F}} \quad (20)$$

where $J^{1/3} \mathbf{I}$ describes the purely volumetric deformation and $\bar{\mathbf{F}}$ captures the isochoric since $|\bar{\mathbf{F}}| = |J^{-1/3} \mathbf{F}| = 1$. Similarly we can decompose right Cauchy-Green tensor

$$\bar{\mathbf{C}} = \bar{\mathbf{F}}^T \bar{\mathbf{F}} = J^{-2/3} \mathbf{C} \quad (21)$$

where $\bar{\mathbf{F}}$ and $\bar{\mathbf{C}}$ are known as the modified deformation gradient and modified right Cauchy-Green tensor, respectively. Moreover, the modified principal stretches $\bar{\lambda}_i$ and modified invariants $\bar{\mathbb{I}}_i$ can be defined

$$\bar{\lambda}_i = J^{-1/3} \lambda_i, \quad i = 1, 2, 3 \quad (22)$$

$$\bar{\mathbb{I}}_1 = J^{-2/3} \mathbb{I}_1, \quad \bar{\mathbb{I}}_2 = J^{-4/3} \mathbb{I}_2, \quad \bar{\mathbb{I}}_3 = (J^{-2/3})^3 \mathbb{I}_3 = 1. \quad (23)$$

The general decoupled strain energy is a sum of volumetric and isochoric parts

$$\psi(J, \bar{\mathbf{C}}) = \psi_{\text{vol}}(J) + \psi_{\text{iso}}(\bar{\mathbf{C}}), \quad (24)$$

leading to an additive decomposition of the second Piola-Kirchhoff stress

$$\mathbf{S} = \frac{\partial \psi}{\partial \mathbf{E}} = \frac{\partial \psi_{\text{vol}}}{\partial J} \frac{\partial J}{\partial \mathbf{E}} + \frac{\partial \psi_{\text{iso}}}{\partial \mathbf{E}} = \mathbf{S}_{\text{vol}} + \mathbf{S}_{\text{iso}}. \quad (25)$$

When the isochoric strain energy is written in terms of modified invariants $\psi_{\text{iso}}(\bar{\mathbb{I}}_1, \bar{\mathbb{I}}_2)$ (note that $\bar{\mathbb{I}}_3 = 1$ uniformly), the isochoric stress satisfies

$$\mathbf{S}_{\text{iso}} = \frac{\partial \psi_{\text{iso}}}{\partial \mathbf{E}} = 2 \frac{\partial \psi_{\text{iso}}}{\partial \bar{\mathbf{C}}} = 2 \sum_{i=1}^3 \frac{\partial \psi_{\text{iso}}}{\partial \bar{\mathbb{I}}_i} \frac{\partial \bar{\mathbb{I}}_i}{\partial \bar{\mathbf{C}}} \quad (26)$$

with

$$\begin{aligned} \frac{\partial \bar{\mathbb{I}}_1}{\partial \bar{\mathbf{C}}} &= \frac{\partial (J^{-2/3} \mathbb{I}_1)}{\partial \bar{\mathbf{C}}} = J^{-2/3} \left(\mathbf{I}_3 - \frac{1}{3} \mathbb{I}_1 \mathbf{C}^{-1} \right) \\ \frac{\partial \bar{\mathbb{I}}_2}{\partial \bar{\mathbf{C}}} &= \frac{\partial (J^{-4/3} \mathbb{I}_2)}{\partial \bar{\mathbf{C}}} = J^{-4/3} \left(\mathbb{I}_1 \mathbf{I}_3 - \mathbf{C} - \frac{2}{3} \mathbb{I}_2 \mathbf{C}^{-1} \right), \end{aligned} \quad (27)$$

where we have used $\frac{\partial J}{\partial \mathbf{C}} = \frac{1}{2} J \mathbf{C}^{-1}$. As discussed for (9), there are many empirical forms for the pure volumetric part (or bulk term) of the strain-energy, which should be convex and satisfy physical constraints^{16,17}. We consider one such form,

$$\psi_{\text{vol}} = \frac{k}{4} (J^2 - 1 - 2 \log J), \quad (28)$$

but similar principles will give stable formulations for others. The volumetric stress can be defined as

$$\mathbf{S}_{\text{vol}} = -p \frac{\partial J}{\partial \mathbf{E}} = -p J \mathbf{C}^{-1} \quad (29)$$

where we have used the definition of hydrostatic pressure $p = -\frac{\partial \psi_{\text{vol}}}{\partial J}$, which for (28) can be stably computed via

$$p = -\frac{k}{2J} (J^2 - 1) = -\frac{k}{2J} J_{-1} (J_{-1} + 2). \quad (30)$$

While p depends on the form $\psi_{\text{vol}}(J)$, the volumetric stress (29) is numerically stable and always the same expression in terms of p . In the decoupled framework, the only salient difference between the Neo-Hookean, Mooney-Rivlin, and Ogden models is in their isochoric part, thus we focus on stable expressions for isochoric stresses \mathbf{S}_{iso} and $\boldsymbol{\tau}_{\text{iso}}$.

2.2.1 | Neo-Hookean model

The decoupled strain energy density for the Neo-Hookean model is

$$\psi(J, \bar{\mathbf{C}}) = \psi_{\text{vol}}(J) + \frac{\mu}{2} (\bar{\mathbb{I}}_1 - 3) \quad (31)$$

The isochoric second Piola-Kirchhoff stress is a straightforward application of (27),

$$\mathbf{S}_{\text{iso}} = \mu J^{-2/3} \left(\mathbf{I} - \frac{1}{3} \mathbb{I}_1 \mathbf{C}^{-1} \right). \quad (32)$$

Using the relation $\mathbb{I}_1(\mathbf{C}) = 3 + 2\mathbb{I}_1(\mathbf{E})$, the numerically stable form of (32) can be written as

$$\mathbf{S}_{\text{iso}} = 2\mu J^{-2/3} \mathbf{C}^{-1} \left(\mathbf{E} - \frac{1}{3} \mathbb{I}_1(\mathbf{E}) \mathbf{I} \right) = 2\mu J^{-2/3} \mathbf{C}^{-1} \mathbf{E}_{\text{dev}}, \quad (33)$$

which makes use of the deviatoric Green-Lagrange strain $\mathbf{E}_{\text{dev}} = \mathbf{E} - \frac{1}{3} \mathbb{I}_1(\mathbf{E}) \mathbf{I}$.

In current configuration, the isochoric Kirchhoff stress is

$$\boldsymbol{\tau}_{\text{iso}} = \mathbf{F} \mathbf{S}_{\text{iso}} \mathbf{F}^T = \mu J^{-2/3} \left(\mathbf{b} - \frac{1}{3} \mathbb{I}_1(\mathbf{b}) \mathbf{I} \right) \quad (34)$$

and its equivalent stable form is

$$\boldsymbol{\tau}_{\text{iso}} = 2\mu J^{-2/3} \left(\mathbf{e} - \frac{1}{3} \mathbb{I}_1(\mathbf{e}) \mathbf{I} \right) = 2\mu J^{-2/3} \mathbf{e}_{\text{dev}}, \quad (35)$$

where we have used $\mathbb{I}_1(\mathbf{b}) = 3 + 2\mathbb{I}_1(\mathbf{e})$.

2.2.2 | Mooney-Rivlin model

For the Mooney-Rivlin model, decoupled strain energy density is given by

$$\psi(J, \bar{\mathbf{C}}) = \psi_{\text{vol}}(J) + \frac{\mu_1}{2} (\bar{\mathbb{I}}_1 - 3) + \frac{\mu_2}{2} (\bar{\mathbb{I}}_2 - 3) \quad (36)$$

The isochoric second Piola-Kirchhoff stress can be written as (27)

$$\mathbf{S}_{\text{iso}} = \mu_1 J^{-2/3} \left(\mathbf{I} - \frac{1}{3} \mathbb{I}_1(\mathbf{C}) \mathbf{C}^{-1} \right) + \mu_2 J^{-4/3} \left(\mathbb{I}_1(\mathbf{C}) \mathbf{I} - \mathbf{C} - \frac{2}{3} \mathbb{I}_2(\mathbf{C}) \mathbf{C}^{-1} \right) \quad (37)$$

and its stable form is

$$\begin{aligned} \mathbf{S}_{\text{iso}} &= 2\mu_1 J^{-2/3} \mathbf{C}^{-1} \left(\mathbf{E} - \frac{1}{3} \mathbb{I}_1(\mathbf{E}) \mathbf{I} \right) + 2\mu_2 J^{-4/3} (\mathbb{I}_1(\mathbf{E}) \mathbf{I} - \mathbf{E}) + 4\mu_2 J^{-4/3} \mathbf{C}^{-1} \left(\mathbf{E} - \frac{2}{3} \mathbb{I}_1(\mathbf{E}) \mathbf{I} - \frac{2}{3} \mathbb{I}_2(\mathbf{E}) \mathbf{I} \right) \\ &= 2 (\mu_1 J^{-2/3} + 2\mu_2 J^{-4/3}) \mathbf{C}^{-1} \mathbf{E}_{\text{dev}} + 2\mu_2 J^{-4/3} (\mathbb{I}_1(\mathbf{E}) \mathbf{I} - \mathbf{E}) - \frac{4}{3} \mu_2 J^{-4/3} (\mathbb{I}_1(\mathbf{E}) + 2\mathbb{I}_2(\mathbf{E})) \mathbf{C}^{-1}, \end{aligned} \quad (38)$$

where we have used $\mathbb{I}_1(\mathbf{C}) = 3 + 2\mathbb{I}_1(\mathbf{E})$, $\mathbb{I}_2(\mathbf{C}) = 3 + 4\mathbb{I}_1(\mathbf{E}) + 4\mathbb{I}_2(\mathbf{E})$.

In current configuration we have

$$\boldsymbol{\tau}_{\text{iso}} = \mu_1 J^{-2/3} \left(\mathbf{b} - \frac{1}{3} \mathbb{I}_1(\mathbf{b}) \mathbf{I} \right) + \mu_2 J^{-4/3} \left(\mathbb{I}_1(\mathbf{b}) \mathbf{b} - \mathbf{b}^2 - \frac{2}{3} \mathbb{I}_2(\mathbf{b}) \mathbf{I} \right) \quad (39)$$

and the stable form of (39) is

$$\begin{aligned} \boldsymbol{\tau}_{\text{iso}} &= 2\mu_1 J^{-2/3} \left(\mathbf{e} - \frac{1}{3} \mathbb{I}_1(\mathbf{e}) \mathbf{I} \right) + 2\mu_2 J^{-4/3} (\mathbb{I}_1(\mathbf{e}) \mathbf{I} - \mathbf{e}) + 4\mu_2 J^{-4/3} \left(\mathbf{e} - \frac{2}{3} \mathbb{I}_1(\mathbf{e}) \mathbf{I} - \frac{2}{3} \mathbb{I}_2(\mathbf{e}) \mathbf{I} \right) \\ &= 2 (\mu_1 J^{-2/3} + 2\mu_2 J^{-4/3}) \mathbf{e}_{\text{dev}} + 2\mu_2 J^{-4/3} (\mathbb{I}_1(\mathbf{e}) \mathbf{I} - \mathbf{e}) - \frac{4}{3} \mu_2 J^{-4/3} (\mathbb{I}_1(\mathbf{e}) + 2\mathbb{I}_2(\mathbf{e})) \mathbf{I} \end{aligned} \quad (40)$$

where we have used $\mathbb{I}_1(\mathbf{b}) = 3 + 2\mathbb{I}_1(\mathbf{e})$, $\mathbb{I}_2(\mathbf{b}) = 3 + 4\mathbb{I}_1(\mathbf{e}) + 4\mathbb{I}_2(\mathbf{e})$.

2.2.3 | Ogden model

The postulated decoupled strain energy for Ogden model is a function of the modified principal stretches (22) as^{4,14}

$$\psi(J, \bar{\lambda}_i) = \psi_{\text{vol}}(J) + \psi_{\text{iso}}(\bar{\lambda}_i) = \psi_{\text{vol}}(J) + \sum_{i=1}^3 \bar{\omega}(\bar{\lambda}_i) \quad \text{with} \quad \bar{\omega}(\bar{\lambda}_i) = \sum_{j=1}^N \frac{\mu_j}{\alpha_j} (\bar{\lambda}_i^{\alpha_j} - 1) \quad (41)$$

where the parameters μ_j and α_j have to be determined from experiments. In the linearized regime, all hyperelastic models reduce to linear elasticity, where the shear modulus μ satisfies

$$2\mu = \sum_{j=1}^N \mu_j \alpha_j \quad \text{with} \quad \mu_j \alpha_j > 0 \quad (42)$$

in terms of the Ogden parameters. The isochoric second Piola-Kirchhoff stress can be written as

$$\mathbf{S}_{\text{iso}} = 2 \frac{\partial \psi_{\text{iso}}(\bar{\lambda}_i)}{\partial \mathbf{C}} = \sum_{i=1}^3 2 \frac{\partial \psi_{\text{iso}}}{\partial \lambda_i^2} \frac{\partial \lambda_i^2}{\partial \mathbf{C}} = \sum_{i=1}^3 \frac{1}{\lambda_i} \frac{\partial \psi_{\text{iso}}}{\partial \lambda_i} \mathbf{N}_i \mathbf{N}_i^T = \sum_{i=1}^3 s_i \mathbf{N}_i \mathbf{N}_i^T \quad (43)$$

where an eigenvector \mathbf{N}_i is computed by $\mathbf{C} \mathbf{N}_i = \lambda_i^2 \mathbf{N}_i$. By employing $\frac{\partial J}{\partial \lambda_i} = J \lambda_i^{-1}$ we have

$$s_i = \frac{1}{\lambda_i} \frac{\partial \psi_{\text{iso}}}{\partial \lambda_i} = \frac{1}{\lambda_i} \frac{\partial \bar{\lambda}_k}{\partial \lambda_i} \frac{\partial \psi_{\text{iso}}}{\partial \bar{\lambda}_k} = \frac{J^{-1/3}}{\lambda_i} \left(\delta_{ik} - \frac{1}{3} \lambda_i^{-1} \lambda_k \right) \frac{\partial \psi_{\text{iso}}}{\partial \bar{\lambda}_k} = \frac{J^{-1/3}}{\lambda_i} \left(\delta_{ik} - \frac{1}{3} \bar{\lambda}_i^{-1} \bar{\lambda}_k \right) \frac{\partial \psi_{\text{iso}}}{\partial \bar{\lambda}_k} \quad (44)$$

in which

$$\frac{\partial \psi_{\text{iso}}}{\partial \bar{\lambda}_k} = \frac{\partial \bar{\omega}(\bar{\lambda}_k)}{\partial \bar{\lambda}_k} = \sum_{j=1}^N \mu_j \bar{\lambda}_k^{\alpha_j - 1} \quad (45)$$

To derive an equivalent numerically stable form of (43) we rewrite the ψ_{iso} by substituting $\bar{\lambda}_i = J^{-1/3} \lambda_i$ as

$$\psi_{\text{iso}}(\lambda_i) = \sum_{j=1}^N \frac{\mu_j}{\alpha_j} [(\lambda_1^{\alpha_j} + \lambda_2^{\alpha_j} + \lambda_3^{\alpha_j}) J^{-\alpha_j/3} - 3] \quad (46)$$

and computing its derivative as

$$\begin{aligned} s_1 &= \frac{1}{\lambda_1} \frac{\partial \psi_{\text{iso}}}{\partial \lambda_1} = \frac{1}{\lambda_1} \sum_{j=1}^N \frac{\mu_j}{\alpha_j} \left[\left(\alpha_j \lambda_1^{\alpha_j - 1} \right) J^{-\alpha_j/3} - \frac{\alpha_j}{3} J^{-\alpha_j/3} \lambda_1^{-1} (\lambda_1^{\alpha_j} + \lambda_2^{\alpha_j} + \lambda_3^{\alpha_j}) \right] \\ &= \frac{1}{\lambda_1} \sum_{j=1}^N \mu_j \left[\lambda_1^{\alpha_j - 1} - \frac{1}{3} \lambda_1^{-1} (\lambda_1^{\alpha_j} + \lambda_2^{\alpha_j} + \lambda_3^{\alpha_j}) \right] J^{-\alpha_j/3} \\ &= \frac{1}{\lambda_1^2} \sum_{j=1}^N \frac{\mu_j}{3} [2\lambda_1^{\alpha_j} - \lambda_2^{\alpha_j} - \lambda_3^{\alpha_j}] J^{-\alpha_j/3} \\ &= \frac{1}{\lambda_1^2} \sum_{j=1}^N \frac{\mu_j}{3} [2(\lambda_1^{\alpha_j} - 1) - (\lambda_2^{\alpha_j} - 1) - (\lambda_3^{\alpha_j} - 1)] J^{-\alpha_j/3} \\ &= \frac{1}{\lambda_1^2} \sum_{j=1}^N \frac{\mu_j}{3} [2(e^{\alpha_j \ell_1} - 1) - (e^{\alpha_j \ell_2} - 1) - (e^{\alpha_j \ell_3} - 1)] J^{-\alpha_j/3} \\ &= \frac{1}{1 + 2\lambda_1^E} \sum_{j=1}^N \frac{\mu_j}{3} [2 \expm1(\alpha_j \ell_1) - \expm1(\alpha_j \ell_2) - \expm1(\alpha_j \ell_3)] J^{-\alpha_j/3} \end{aligned} \quad (47)$$

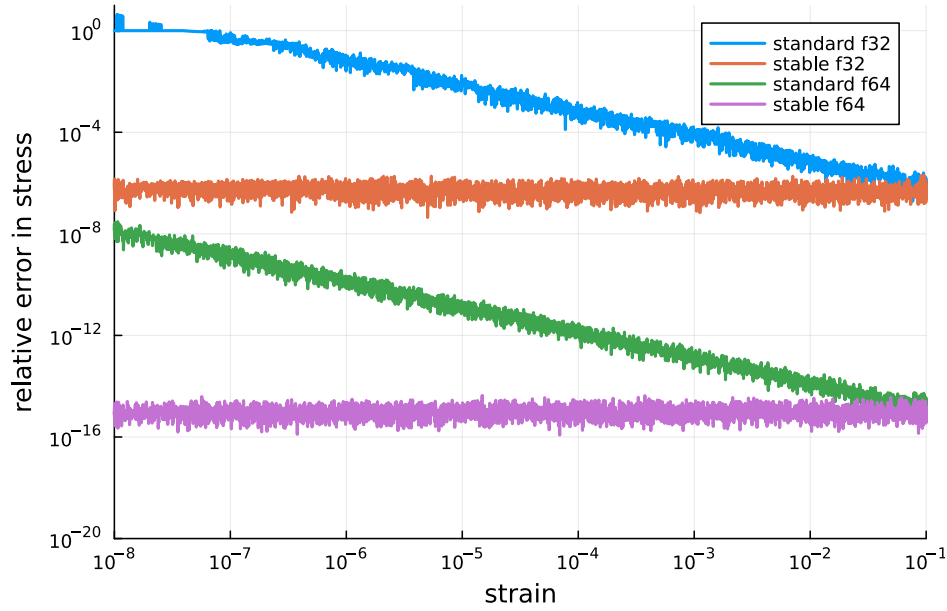


FIGURE 3 Relative error of standard computation of isochoric second Piola-Kirchhoff stress for Ogden model and its stable form

where λ_i^E is the eigenvalue of strain tensor \mathbf{E} and $\ell_i = \log \lambda_i = \frac{1}{2} \log_{10}(2\lambda_i^E)$. Following the above approach we have

$$\begin{aligned} s_2 &= \frac{1}{\lambda_2} \frac{\partial \psi_{\text{iso}}}{\partial \lambda_2} = \frac{1}{1 + 2\lambda_2^E} \sum_{j=1}^N \frac{\mu_j}{3} [-\expm1(\alpha_j \ell_1) + 2 \expm1(\alpha_j \ell_2) - \expm1(\alpha_j \ell_3)] J^{-\alpha_j/3} \\ s_3 &= \frac{1}{\lambda_3} \frac{\partial \psi_{\text{iso}}}{\partial \lambda_3} = \frac{1}{1 + 2\lambda_3^E} \sum_{j=1}^N \frac{\mu_j}{3} [-\expm1(\alpha_j \ell_1) - \expm1(\alpha_j \ell_2) + 2 \expm1(\alpha_j \ell_3)] J^{-\alpha_j/3}. \end{aligned} \quad (48)$$

Substituting the new definition of s_i (47) and (48) into (43) provides a stable form of the isochoric second Piola-Kirchhoff stress for the Ogden model. Relative error for the standard (44) and stable (47)-(48) form of the isochoric second Piola-Kirchhoff stress (43) for the Ogden model is plotted in Figure 3. The behavior for single and double precision is similar to Figure 2.

Note that for symmetric, real-valued 3×3 strain tensor \mathbf{E} , the standard closed-form solutions for eigenvalues are susceptible to loss of significance in floating point computation. Therefore we computed λ_i^E , by the stable algorithm proposed in¹⁸, which has a relative accuracy of $\epsilon_{\text{machine}}$.

2.3 | Hencky strain

Standard material logarithmic or Hencky strain is defined as

$$\mathbf{E}_H = \log(\mathbf{U}) = \frac{1}{2} \log(\mathbf{C}) = \frac{1}{2} \sum_{i=1}^3 \log(\lambda_i) \mathbf{N}_i \mathbf{N}_i^T, \quad (49)$$

which is numerically unstable when $\lambda_i \approx 1$. The stable version can be computed by

$$\mathbf{E}_H = \frac{1}{2} \log(2\mathbf{E} + \mathbf{I}) = \frac{1}{2} \sum_{i=1}^3 \log_{10}(2\lambda_i^E) \mathbf{N}_i \mathbf{N}_i^T. \quad (50)$$

We can use a similar approach to define the stable form of the spatial logarithmic in current configuration

$$\mathbf{e}_H = \log(\mathbf{v}) = \frac{1}{2} \log(\mathbf{b}) \quad (51)$$

by using the \mathbf{e} 's eigenvalues as

$$\mathbf{e}_H = \frac{1}{2} \log(2\mathbf{e} + I) = \frac{1}{2} \sum_{i=1}^3 \log_{1p}(2\lambda_i^e) \mathbf{n}_i \mathbf{n}_i^T. \quad (52)$$

With strain computed in a stable way, constitutive models based on the Hencky strain can stably evaluated using the principles in the prior sections.

3 | ALGORITHMIC DIFFERENTIATION TO DERIVE MATERIAL MODELS

Deriving some of the material models in section 2 is not a trivial task, and could be tedious and error-prone. One way to derive complicated material models without needing to manipulate and simplify the intermediate expressions is to use algorithmic (aka. automatic) differentiation (AD). Starting from the strain energy function in terms of the strain tensor, one could use an AD tool to compute the corresponding stress tensor. However, using AD does not *automatically* guarantee stability. Instabilities in the strain energy function will propagate to the derivatives, leading to an unstable evaluation of stress. Our primary goal here is to show how to compute material models using AD, identify instability-inducing terms in the free energy function, and introducing a stable form of the strain energy function. We chose the coupled Neo-Hookean model (8) to show the procedure. One can apply these principles to obtain stable representations for other material models.

We start with re-writing equation (8) in terms of \mathbf{E} .

$$\psi(\mathbf{E}) = \frac{\lambda}{4} (J^2 - 1 - 2 \log J) - \mu (\log J - \text{trace}(\mathbf{E})), \quad (53)$$

where $J = \sqrt{2\mathbf{E} + I}$. As we saw in (2.1.1), equation (53) is unstable due to the presence of the $J^2 - 1$ and $\log J$ terms. Using (10)-(11), we can transform (53) to

$$\begin{aligned} \psi(\mathbf{E}) &= \frac{\lambda}{4} (\mathbb{J}_{-1} (\mathbb{J}_{-1} + 2) - 2 \log_{1p} (\mathbb{J}_{-1})) - \mu (\log_{1p} (\mathbb{J}_{-1}) - \text{trace}(\mathbf{E})) \\ &= \frac{\lambda}{4} \left(\underbrace{\mathbb{J}_{-1}^2}_{O(\epsilon^2)} - 2 \underbrace{(\log_{1p} \mathbb{J}_{-1} - \mathbb{J}_{-1})}_{O(\epsilon^2)} \right) - \mu \underbrace{(\log_{1p} \mathbb{J}_{-1} - \text{trace} \mathbf{E})}_{O(\epsilon^2)}. \end{aligned} \quad (54)$$

While (54) is more stable than (53), it is still unstable when $J \approx 1$ and its derivative results in an unstable formulation for stress due to numerical cancellations in the $\log_{1p} \mathbb{J}_{-1} - \mathbb{J}_{-1}$ and $\log_{1p} (\mathbb{J}_{-1}) - \text{trace}(\mathbf{E})$ terms. Looking more closely at these terms, if \mathbf{E} is of scale ϵ , then $\psi(\mathbf{E}) \in O(\epsilon^2)$ and thus we need to avoid subtracting terms such as \mathbb{J}_{-1} and $\text{trace} \mathbf{E}$, which are $O(\epsilon)$. The first underbrace in (54) is fine as is, but the second and third require a reformulation.

For the second underbrace, we define a helper function for computing $\log(1+x) - x$ that avoids subtracting $O(x)$ terms when computing the $O(x^2)$ result. Knowing²

$$\begin{aligned} \log_{1p}(x) &= \log(1+x) \\ &= 2 \operatorname{artanh} \left(\frac{x}{2+x} \right) \\ &= 2 \sum_{n=0}^{\infty} \frac{1}{2n+1} \left(\frac{x}{2+x} \right)^{2n+1}, \quad \left| \frac{x}{2+x} \right| < 1. \end{aligned} \quad (55)$$

and moving x to the left hand side, we have

$$\begin{aligned} \log_{1p_minus_x}(x) &= \log(1+x) - x \\ &= -\frac{x^2}{2+x} + 2 \sum_{n=1}^{\infty} \frac{1}{2n+1} \left(\frac{x}{2+x} \right)^{2n+1}, \quad \left| \frac{x}{2+x} \right| < 1. \end{aligned} \quad (56)$$

Appendix B studies how many terms are necessary to evaluate $\log_{1p_minus_x}$ accurately.

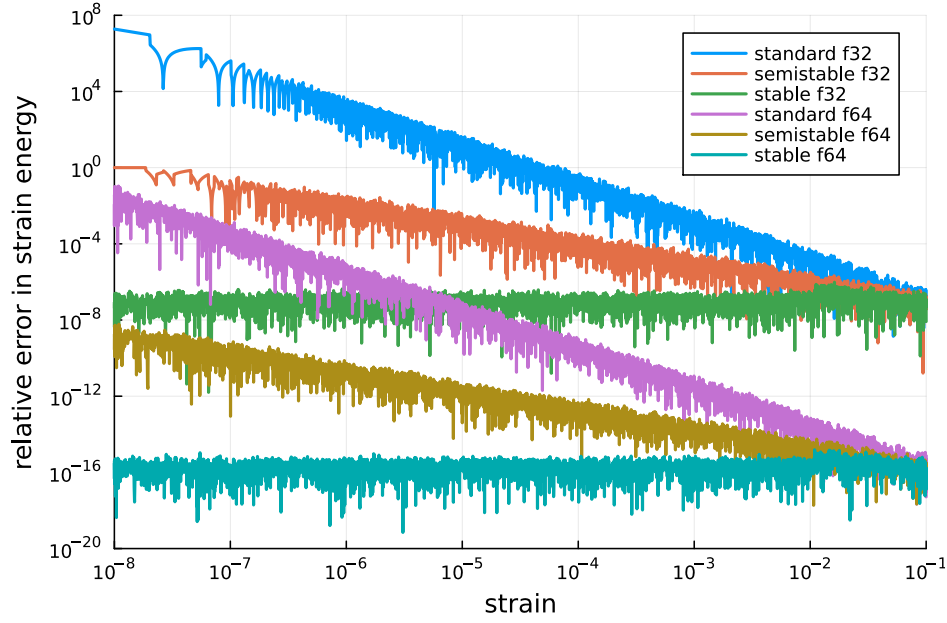


FIGURE 4 Relative error of computation of Neo-Hookean strain energy in standard (53), semistable (54) and stable (60) forms.

With a stable implementation of `loglp_minus_x` available, we need only a stable formulation for the third underbrace in (54). Considering a 2×2 strain tensor, we can break down J^2 into

$$\begin{aligned} J^2 &= |\mathbf{I} + 2\mathbf{E}| \\ &= 1 + 2 \underbrace{(E_{1,1} + E_{2,2})}_{\text{trace}(\mathbf{E})} + 4(E_{1,1}E_{2,2} - E_{1,2}E_{2,1}), \end{aligned} \quad (57)$$

and define a new variable:

$$\begin{aligned} \mathbf{j} &= J^2 - 1 - 2 \text{trace}(\mathbf{E}) \\ &= 4(E_{1,1}E_{2,2} - E_{1,2}E_{2,1}). \end{aligned} \quad (58)$$

Using (58) extended for 3×3 matrices, we can compute J_{-1} as

$$J_{-1} = \frac{J^2 - 1}{J + 1} = \frac{\mathbf{j} + 2 \text{trace}(\mathbf{E})}{J + 1}. \quad (59)$$

Finally, with (56)-(59), we arrive at a stable representation of the strain energy function (53) as

$$\psi(\mathbf{E}) = \frac{\lambda}{4} (J_{-1}^2 - 2 \text{loglp_minus_x}(J_{-1})) - \mu (\text{loglp_minus_x}(\mathbf{j} + 2 \text{trace}(\mathbf{E})) + \mathbf{j}). \quad (60)$$

Figure 4 shows the relative error of strain energy function for Neo-Hookean model. For the strain of order 10^{-8} we lose 16 and 8 digits in the standard (53) and semistable (54) forms, respectively, while the stable form (60) delivers full accuracy.

We can now expect AD tools to automatically generate a stable representation of the second Piola-Kirchhoff stress, $\mathbf{S} = \frac{\partial \psi}{\partial \mathbf{E}}$, and indeed, Figure 5 shows that direct application of Zygote.jl¹⁹ to (60) (with $n = 6$ in (56)) is stable. Meanwhile, the standard and semistable forms both lose 8 digits for strain at order 10^{-8} . Listing 1 shows sample Julia code to compute \mathbf{S} via reverse-mode AD. We note that AD tools that can compute higher derivatives, e.g., by applying forward-mode AD to $\mathbf{S}(\mathbf{E})$, can readily provide ingredients for solvers (such as Newton linearization) and diagnostics, freeing the implementer from tedious coding of higher derivatives or resorting to numerical differentiation.

Listing 1 Code for computing stress \mathbf{S} for an arbitrary strain energy $\psi(\mathbf{E})$ using the AD tool Zygote.jl.

```
using Zygote
```

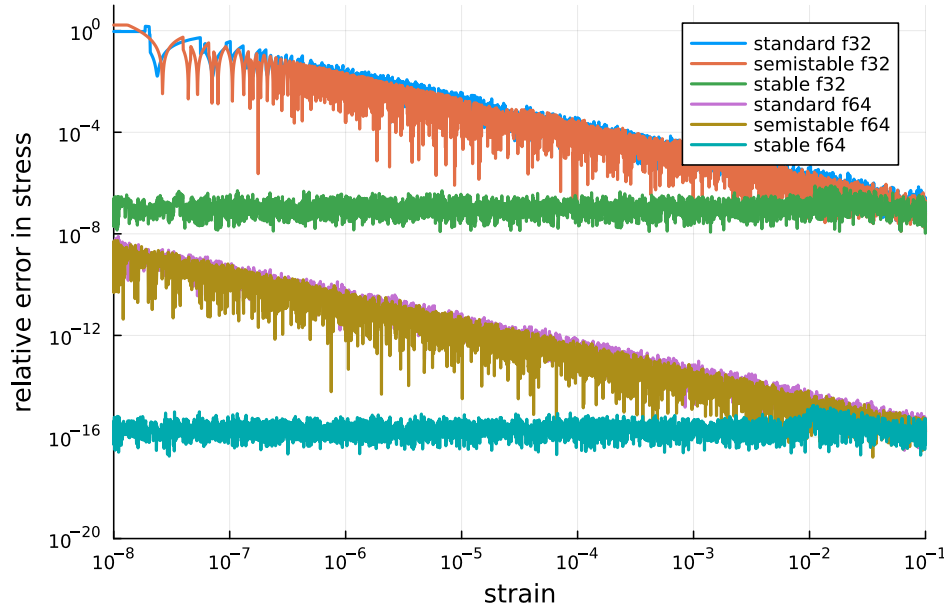


FIGURE 5 Relative error of computation of stress with AD using the standard, semistable and stable forms of strain energy.

```
function S(E, psi)
    stress, = Zygote.gradient(psi, E)
    stress
end
```

4 | CONCLUSIONS

In this paper, we investigated various constitutive formulations for elasticity along with their implementation in finite element software packages. Formulations written in terms of the deformation gradient \mathbf{F} cannot be numerically stable. Standard formulations have additional instabilities due to the presence of function like $J - 1$ and/or $\log J$, which are unstable when $J \approx 1$, as well as terms like $\mathbf{I} - \mathbf{C}^{-1}$, which similarly experience cancellation for small strain $\mathbf{E} \approx 0$. In general, the standard computation for a strain of order 10^{-m} will result in m digits lost in the computed stress tensor and $2m$ lost evaluating the strain energy function. We proposed equivalent stable formulations, all of which achieve relative accuracy $O(\epsilon_{\text{machine}})$. These new formulations make use of the displacement gradient \mathbf{H} to define a strain tensor without loss of significance, compute $J - 1$ in a stable way, and avoid cancellation computing shear stress terms. In addition to coupled and decoupled forms of Neo-Hookean, Mooney-Rivlin, and Ogden models in initial and current configuration, we showed that one can achieve a stable formulation using algorithmic differentiation (AD) if the forward model (strain energy) is stable. We also showed a stable evaluation of Hencky strain, which is important for developing stable representations for inelastic models at finite strain.

With single precision in the standard formulation, the first digit of stress is incorrect for strains of order 10^{-7} , while the new stable formulations get all 7 digits correct at all strain levels. The stable formulations open the door for hyperelastic simulation using single or mixed precision²⁰, thereby improving performance and reducing hardware and energy cost without compromising accuracy. Moreover, stable formulations are necessary to run efficiently on hardware that does not support double precision, such as GPUs, tensor cores, and embedded devices.

REFERENCES

1. Trefethen LN, Bau D. *Numerical Linear Algebra*. Philadelphia, PA: Society for Industrial and Applied Mathematics . 1997
2. Beebe NHF. *The Mathematical-Function Computation Handbook - Programming Using the MathCW Portable Software Library*. Springer . 2017
3. Beebe NH. Computation of $\expm1(x) = \exp(x) - 1$. Online: <https://www.math.utah.edu/~beebe/reports/expm1.pdf>; 2002.
4. Wriggers P. *Nonlinear finite element methods*. Springer Science & Business Media . 2008
5. Taylor RL. FEAP - Finite Element Analysis Program. Online: <http://projects.ce.berkeley.edu/feap/>; 2014.

6. Govindjee S. Personal communication; 2022.
7. Smith M. *ABAQUS/Standard User's Manual, Version 6.9*. United States: Dassault Systèmes Simulia Corp . 2009.
8. Maas SA, Ellis BJ, Ateshian GA, Weiss JA. FEBio: Finite Elements for Biomechanics. *Journal of Biomechanical Engineering* 2012; 134(1): 011005. doi: 10.1115/1.4005694
9. Kaczmarczyk Ł, Ullah Z, Lewandowski K, et al. MoFEM: An open source, parallel finite element library. *Journal of Open Source Software* 2020; 5(45): 1441. doi: 10.21105/joss.01441
10. Lindsay AD, Gaston DR, Permann CJ, et al. 2.0 - MOOSE: Enabling massively parallel multiphysics simulation. *SoftwareX* 2022; 20: 101202. doi: 10.1016/j.softx.2022.101202
11. Salinger AG, Bartlett RA, Bradley AM, et al. Albany: using component-based design to develop a flexible, generic multiphysics analysis code. *International Journal for Multiscale Computational Engineering* 2016; 14(4). doi: 10.1615/IntJMultCompEng.2016017040
12. Bertagna L, Deparis S, Formaggia L, Forti D, Veneziani A. The LifeV library: engineering mathematics beyond the proof of concept. *arXiv math.NA* 2017. doi: 10.48550/arXiv.1710.06596
13. Atkins Z, Brown J, Ghaffari L, Shakeri R, Stengel R, Thompson JL. Ratel User Manual. *Zenodo* 2023. doi: 10.5281/zenodo.10063890
14. Holzapfel G. *Nonlinear solid mechanics: a continuum approach for engineering*. Chichester New York: Wiley . 2000.
15. Shakeri R, Brown J, Ghaffari L, Thompson J, Stengel K. Demo code for stable numerics. *Zenodo* 2024. doi: 10.5281/zenodo.10553116
16. Doll S, Schweizerhof K. On the Development of Volumetric Strain Energy Functions. *Journal of Applied Mechanics* 2000; 67: 17-21. doi: 10.1115/1.321146
17. Moerman KM, Fereidoonzhad B, McGarry JP. Novel hyperelastic models for large volumetric deformations. *International Journal of Solids and Structures* 2020; 193-194: 474-491. doi: 10.1016/j.ijsolstr.2020.01.019
18. Harari I, Albocher U. Computation of eigenvalues of a real, symmetric 3×3 matrix with particular reference to the pernicious case of two nearly equal eigenvalues. *International Journal for Numerical Methods in Engineering* 2023; 124(5): 1089-1110. doi: 10.1002/nme.7153
19. Innes M. Don't Unroll Adjoint: Differentiating SSA-Form Programs. *CoRR* 2018. doi: 10.48550/arXiv.1810.07951
20. Abdelfattah A, Anzt H, Boman EG, et al. A survey of numerical linear algebra methods utilizing mixed-precision arithmetic. *The International Journal of High Performance Computing Applications* 2021; 35(4): 344-369. doi: 10.1177/10943420211003313

□

APPENDIX

A NUMERICAL STABILITY EVALUATION

In order to compare stability of different implementations of functions of the displacement gradient $\mathbf{H} = \frac{\partial \mathbf{u}}{\partial \mathbf{X}}$, we start with by sampling \mathbf{H} as the absolute value of a standard normal distribution ($\mathbf{H} = \text{abs} . (\text{randn}(3, 3))$ in Julia) and then plot relative error of each function $f(\epsilon \mathbf{H})$ as in Listing 2, where $\epsilon \in (10^{-8}, 10^{-1})$ to cover a range from small to large strain. Julia's `big` converts the input to arbitrary precision (default gives $\epsilon_{\text{machine}} < 10^{-77}$) and further operations retain that arbitrary precision. For the range of ϵ considered, the `big` arithmetic can be considered exact. reference and then calculate the relative error for single and double precision i.e., `repr = Float32` and `repr = Float64`.

Listing 2 Julia code for computing relative error of function $f(\epsilon \mathbf{H})$

```
function rel_error(eps, f, repr)
    ref = f(big.(eps*H)) # arbitrary precision
    norm(f(repr.(eps*H)) - ref) / norm(ref)
end
```

We start with the $J - 1$ term which appears in all hyperelastic models and compare it with its stable form \mathbb{J}_{-1} (10) as defined in Julia in Listing 3 and their relative errors are shown in figure (2). As expected, the stable computation \mathbb{J}_{-1} has a relative accuracy of order $\epsilon_{\text{machine}}$ for single and double precision and $J - 1$ loses accuracy as \mathbf{H} decreases. In fact, for $u_{i,j}$ of order 10^{-8} we can trust no digits in single precision and we lost half of the digits in double precision, respectively.

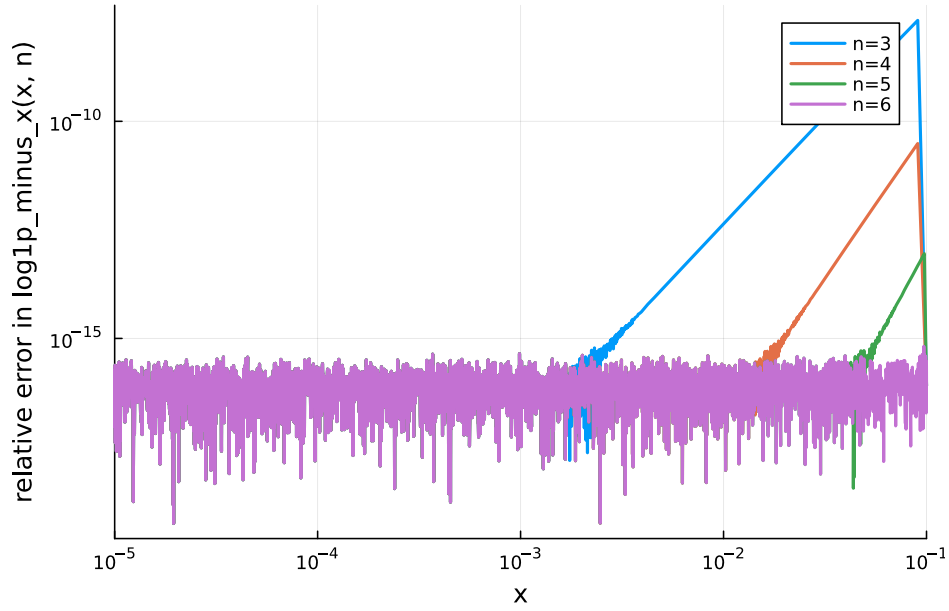


FIGURE B1 Relative error of computation of `log1p_minus_x()` for different expansions of the Taylor series.

Listing 3 Code for computing $J - 1$ and J_{-1}

```
function Jm1_unstable(H)
    F = I + H
    J = det(F)
    J - 1
end

function Jm1_stable(H)
    det_H = det(H)
    A1 = H[1,1]*H[2,2] + H[1,1]*H[3,3] + H[2,2]*H[3,3]
    A2 = H[1,2]*H[2,1] + H[1,3]*H[3,1] + H[2,3]*H[3,2]
    # Compute J-1
    det_H + tr(H) + A1 - A2
end
```

To assess stability of constitutive models, we implement the standard and unstable expressions for the appropriate stress $S(\mathbf{H})$ or $\tau(\mathbf{H})$, internally making use of Green-Lagrange or Green-Euler strains computed by stable means (3), and measure the relative error via Listing 2, yielding figures like Figure 3 and Figure 5.

B ACCURATE EVALUATION OF `log1p_minus_x`

We require efficient and accurate evaluation of the function $\text{log1p_minus_x}(x) = \log(1+x) - x$ to ensure accuracy of the AD-computed stresses in section 3. Figure B1 demonstrates that $n = 6$ in (56) is sufficient to provide $O(\epsilon_{\text{machine}})$ accuracy evaluating $\text{log1p_minus_x}(x)$ for $\epsilon \in (10^{-5}, 10^{-1})$. We believe it would be fruitful to develop a uniformly accurate algorithm for `log1p_minus_x` and include it in numerical libraries.